IEEE Photonics Journal
An IEEE Photonics Society Publication

Open Access

Multi-Hop Relay Based Free Space Optical Communication Link for Delivering Medical Services in Remote Areas

Volume 12, Number 4, August 2020

Rajan Miglani
Jagjit Singh Malhotra
Arun K. Majumdar
Faisel Tubbal
Raad Raad

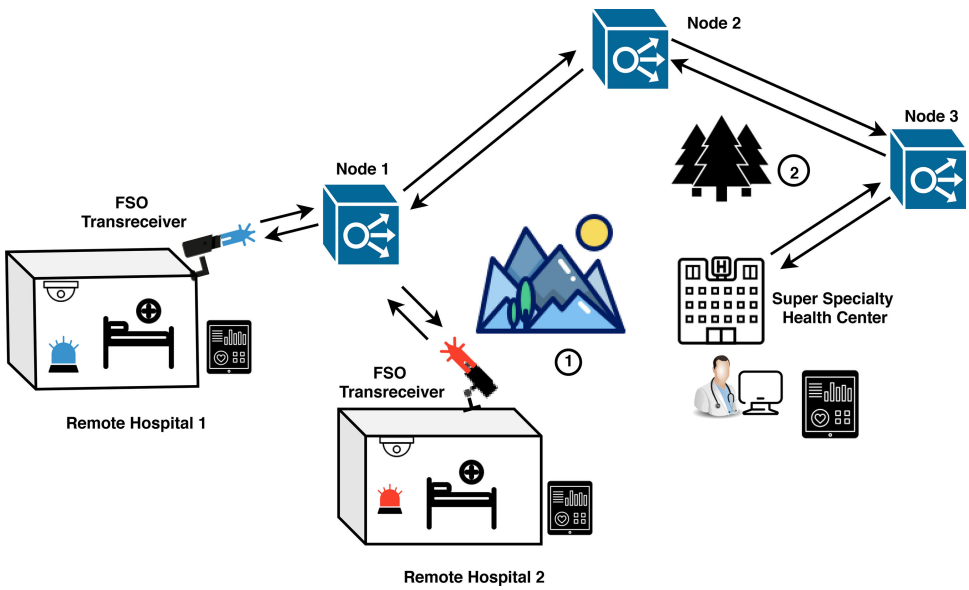

DOI: 10.1109/JPHOT.2020.3013525

Multi-Hop Relay Based Free Space Optical Communication Link for Delivering Medical Services in Remote Areas

Rajan Miglani [1,2] **Jagjit Singh Malhotra, Arun K. Majumdar** [3] **Faisel Tubbal** [4] **and Raad Raad** [5,6]

[1]I. K. G-Punjab Technical University, Punjab 144603, India
[2]Lovely Professional University, Punjab 144411, India
[3]DAV Institute of Engineering and Technology, Punjab 144008, India
[4]Adjunct Professor, Colorado State University, Pueblo, Colorado 81001 USA
[5]School of Electrical, Computer and Telecommunication Engineering, University of Wollongong, Wollongong, NSW 2522, Australia
[6]Technological Projects Department, The Libyan Center for Remote Sensing and Space Science, Tripoli 21218, Libya
[7]School of Electrical, Computer and Telecommunication Engineering, University of Wollongong, Wollongong, NSW 2522, Australia

DOI:10.1109/JPHOT.2020.3013525

Manuscript received July 22, 2020; accepted July 28, 2020. Date of publication July 31, 2020; date of current version August 18, 2020. Corresponding author: Rajan Miglani (e-mail: rajanmiglani1028@gmail.com).

Abstract: Free Space Optical (FSO) communication links are although extremely vulnerable to atmospheric adversities, multi-hop relay transmission can however, significantly improve the link performance and reliability. This paper proposes 120 Gbps DP-16 QAM modulated multi-hop serial FSO link with coherent reception for delivering medical consultation services in remote and isolated locations. Considering the current situation wherein pandemic of highly infectious nature, COVID-19 has affected millions of people globally; doctors can use the proposed high-speed architecture for "contact-less" supervision of quarantined patients and suspects through video conferencing. Each relay terminal uses an all-optical amplify-and-forward technique with Erbium-doped fiber amplifier (EDFA) and gain optimization as its core elements. As a possible last-mile application for delivering medical/health care services, the proposed link has been evaluated for reliability by exposing the link to varied atmospheric conditions. Our results reveal that at target BER of 10^{-5}, the useful communication link range of proposed multi-hop link increments by 1.8 kms as compared to direct link that operates under similar channel conditions. Furthermore, compared to results from recent literature on high-speed FSO [30], the proposed link shows enhancement in link range by approximately 0.7 km. The analysis also reveals that as the number of relay nodes increases, the error performance of the link for different atmospheric conditions approaches a state of convergence.

Index Terms: Atmospheric turbulence, amplify-and-forward relaying, coherent FSO reception, digital signal processing, last-mile connectivity.

1. Introduction

1.1 Preliminaries

Free space optical communication, often addressed synonymously as optical wireless communication, has received massive attention in recent years as a possible alternative to address the issue of last-mile connectivity. High transmission rates, license-free spectrum, easy deployment/relocation,

Fig. 1. Multi-hop FSO link with serial relay configuration.

and unmatched data security are some of the key features that have aroused massive research interest in FSO communication systems, see [1]–[3]. Ever-increasing hunger for high-speed data access has created an urgent need to identify alternative options as the existing radio frequency (RF) regime will be incapable of catering to this demand, see [4]–[6]. Since FSO technology principally shares a technological legacy with the optical fiber communication, hence FSO links are capable of delivering bandwidth that is ideally higher than the existing RF regime by two orders of magnitude, see [7]–[8]. It is for the same reason that the amalgamation of existing optical fiber networks with optical wireless links will not only be convenient but also evolve as a cost-effective solution in delivering optical bandwidth to end-users, see [4], [6], [9].

It is interesting to mention here that necessary hardware components facilitating convergence between fiber and wireless optical links such as free-space optical communication terminals (FSOT) have already made their way into the markets, see [9]–[10]. Despite an array of fascinating features and possible futuristic applications, large scale commercial deployment still eludes FSO systems. This is primarily because the performance of FSO links exhibit weighty dependence on channel conditions, which in turn are dependent on atmospheric conditions, viz. attenuation, and turbulence, see [11]–[12]. Associated with the occurrence of meteorological phenomena like rain, fog, snow, haze, and smog, atmospheric attenuation can have a disastrous effect on link reliability. Furthermore, even when there are no visible signs of aforementioned atmospheric adversities, atmospheric turbulence can still impair the link, see [4]. Caused due to inhomogenities in the refractive index of the medium, atmospheric turbulence causes induced signal fading and this effect magnifies for FSO links with longer link ranges, see [13]. Turbulence induced signal fading can thus limit the useful range to a few hundred meters and, at times, lead to complete link failure, see [11]–[13].

Various techniques like aperture averaging, spatial diversity, special modulation schemes, error coding, adaptive optics (AO) and multi-hop transmission, see [1]–[3], [7]–[9], [13]–[18] have been proposed in recent literature to mitigate channel induced losses in FSO links. Since the atmospheric attenuation and turbulence are distance-dependent factors, see [2], [4], multi-hop transmission smartly transforms this challenge into an opportunity. This is accomplished by dividing the communication link into segments of smaller spans. Since the transmitted signal now passes through intermediate relay nodes instead of a longer direct link, thus largely limiting the effect of attenuation and signal fading.

Fig. 1 highlights the serial relay multi-hop FSO link wherein the transmitter is represented as Source (**S**) and receiver as Destination (**D**), separated by equidistantly placed two relay terminals (**R1** and **R2**). Using multi-hop transmission as the underlying architecture, Fig. 2 demonstrates a possible community-oriented application of multi-hop FSO links which can be successfully used to cater to the medical and health care needs of people living in remote/inaccessible locations. The proposed application connects a super specialty hospital to remote health centers through low cost and high capacity bi-directional FSO links. In developing and under-developing countries, scarcity of resources inhibits the delivery of specialized medical facilities to far-flung areas. Also, in circumstances where an epidemic of highly communicable nature spreads out (e.g., the pandemic of COVID-19), isolation centers to protect other patients and the mainstream population become extremely necessary to prevent disastrous outbreaks. In such cases, a centralized medical facility through the proposed optical wireless links can supervise and prescribe the staff working at remote centers about medical procedures to be followed. The proposed architecture in Fig. 2 illustrates

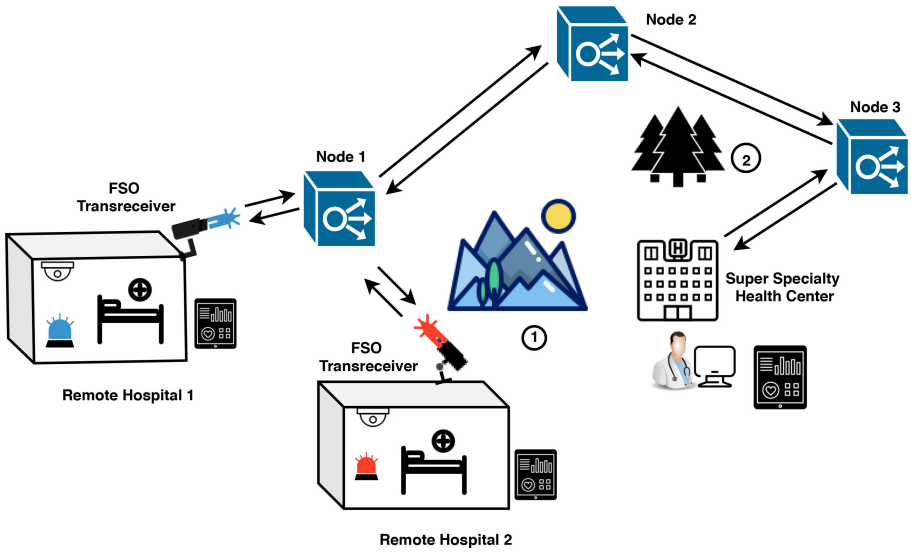

Fig. 2. Proposed health care system to supervise medical prescriptions at remote centers through bi-directional multi-hop link.

another distinct feature of multi-hop links to connect super specialty hospital with two remote health centers, bypassing geographical obstructions labeled 1 (e.g., mountains) and 2 (e.g., trees).

Although FSO links with both parallel and serial relaying have been reported in the literature, the serial configuration is by enlarge considered more dependable. This is because the line-of-sight condition in FSO systems mandates strict transmitter-receiver alignment which will be otherwise quite complex to maintain in parallel relay links, see [19]–[20]. Additionally, it has been reported in, see [21] that parallel relaying does not refine the performance in FSO links especially when operated at low transmission power. Apart from the classification on the basis of relay alignment, multi-hop links can be further classified on the rationale of signal processing inside the relay nodes. Based on signal processing, the nodes can either operate as amplify-and-forward (A-F) or decode-and-forward (D-F) terminal. Furthermore, using the amplification principle as a criterion, the relays can be either all-optical or electrical type nodes.

1.2 Related Literature

Comparison of amplification traits of Erbium-doped fiber amplifier (EDFA) and semiconductor optical amplifier (SOA) for 1 Gbps multi-hop FSO link can be found in, see [7] where the authors, Nor *et al.* proposed two important conclusions. Firstly, in contrast to direct links, relay FSO links yield improved performance for different channel conditions, and secondly, in terms of choice of amplification, all-optical relay nodes outperform electrical amplification. Similarly, authors in, see [13] have also iterated the success of EDFA based multi-hop strategy over direct links in limiting the effect of channel induced losses. However, it has also been flagged herein, see [13] that cascaded stages of the optical amplifier (EDFA) can lead to the accumulation of amplified spontaneous emission (ASE) noise in serial relay transmission. Kazemlou *et al.* in their work on 10 Gbps serial relay link, see [14] demonstrated 40% increment in link range when the direct link was replaced with equidistant serial nodes. It was also concluded here that although regeneration based relay transmission is more reliable than amplify-and-forward relays, the former strategy, however, increases implementation complexity and costs. Performance of EDFA based relays has also been detailed in, see [22] wherein the authors, Bayaki *et al.* presented an analysis on FSO link performance in the presence of adverse weather and turbulent link conditions. Authors

here, see [22], have an opinion that electrical relays not only lead to design complexities but also performance degradation due to noise accumulation at each relay stage.

Safari *et al.*, in their research, see [15], favored serial transmission for FSO links over parallel links, especially if the number of intermediate nodes is higher. All-optical relaying also finds mention in research works of, see [19]–[20] wherein authors have used OptiSystem to design and investigate the performance of multi-hop FSO links over fading channel conditions. Libich *et al.* and Nor *et al.* in their research work, see [23] and [24] respectively, have experimentally proved the practicality of 10 Gbps serial relay FSO transmission over direct links in the presence of turbulent fading conditions. Based on available research findings presented here, we have narrowed down to propose an all-optical amplify and forward (A-F) based multi-hop serial relay FSO link. This choice can be attributed to the fact that both decode-and-forward (D-F) and electrical relay nodes convert the incoming optical signals into an electrical domain followed by signal conditioning measures, viz. signal regeneration and amplification. The regenerated signal is then reconverted to an optical form before relaying it further through the atmospheric channel. From the available literature we may deduce that performance of D-F/electrical relay nodes is limited by: *(i)* necessity of optical to electrical *(O-E)* and vice-versa conversions at each node, thus introducing significant hardware complexities, *(ii)* signal conditioning at each node causes appreciable time delay due to *O-E* and *E-O* conversions, and *(iii)* at high data rates (*Gbps*), electrical signal conditioning inside relay nodes will be a formidable task, see [9], [13]–[15].

1.3 Problem Statement

The *critical* aspect in the success of futuristic communication technologies and standards will be determined by the ease of their convergence with existing high-speed access networks, see [25]–[28]. In this direction it will be critical to highlight the works of, see [9], [28]–[29], where authors have put forward the idea of complimenting FSO systems with wavelength division multiplexing (WDM) to attain twin goals. Firstly, WDM is already a mature technology that has been widely used for capacity enhancement in conventional fiber links. Secondly, WDM-FSO technology can also improvise convergence between FSO systems and the existing network hardware technology. Different research works have been published in the recent past suggesting various strategies in the direction of capacity enhancement in FSO links [9]. While Kakati *et al.* in their research work, see [30]–[31] have used DP-16 QAM to support high data rate transmission, authors in, see [32]–[37] advocate use of wavelength division multiplexing as a more practical approach in achieving transmission rates as high as 1 Tbps. Malik *et al.* and Grover *et al.* in their reported research, see [34] and [35] respectively, proposed a long haul FSO link wherein the transmission powers is 40 dBm while link attenuation is as low as 0.065 dB/km. The high capacity FSO link proposed in, see [36] also follows a similar strategy for capacity enhancement, but the reported link has been investigated without considering the effect of the fading channel. Since it is a well-known fact that transmission power and bandwidth share an inverse proportionality see [37], hence designing FSO links to operate at high data rates while using high transmission power will surely be a practical challenge. Additionally, if FSO systems are to be projected as last-mile technology, then it is important that adverse impact of fading channel on link performance is minimized through smart measures such as relaying. Lastly, to ensure seamless and cost effective delivery of optical bandwidth to end-users, all-optical signal processing based FSO links will play a crucial role.

1.4 Proposed Solution

Through literature gaps reported in the previous section, the authors feel motivated to propose and design a multi-hop FSO link which should: *(i)* deliver high speed data transmission through optical processing of signals at relay nodes, while considering practical constraints of trade-off between bandwidth and power, *(ii)* be capable of delivering requisite performance over an array of meteorological and fading conditions, *(iii)* achieve power and gain optimization at relay nodes

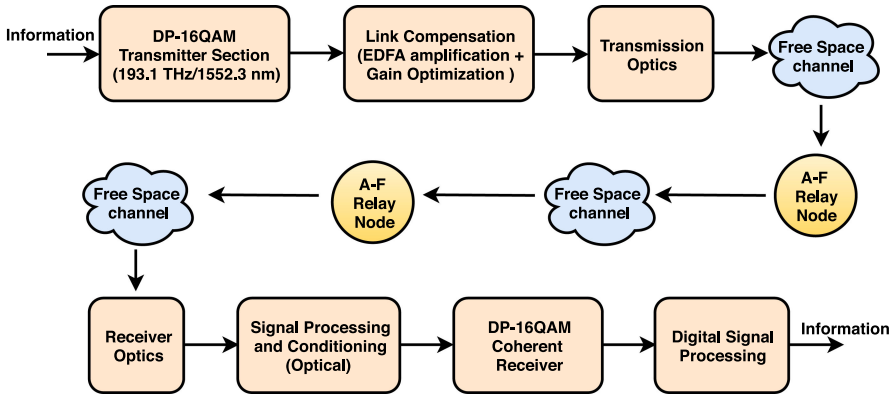

Fig. 3. Block diagram showing transmitter section and receiver section of proposed link.

to overcome limitations of noise accumulation due optical amplification. Considering the aforementioned research gaps, amplify-and-forward (A-F) based all-optical multi-hop serial relay FSO link operating under fading channel has been proposed and investigated here. At each node, the signal processing is accomplished in the high-speed optical domain without any need for complex electrical or optoelectronic processing. The proposed link has been designed, investigated and validated using specialized design tool, OptiSystem.

The rest of the paper has been organized as follows: Section 2 provides insight into link design and signal transmission principles using serial relay mechanism. Section 3 analyses the performance of the proposed link for varied link conditions using bit error rate, link range, and constellation diagram patterns while Section 5 concludes the paper with possible future directions to extend the scope of reported research work.

2. System Model

2.1 Modulation Theory

Intensity-modulation and direct-detection modulation (IM/ DD) schemes are based on modulation of optical source by information signal and thereafter direct demodulation of optical carrier using photodetectors to retrieve the information. Ease and low-cost implementation have been the key reasons for the popularity of IM/DD schemes in FSO systems. However, in the presence of atmospheric adversities, IM/DD FSO links experience degraded reliability and a sharp reduction in operational range, see [5]. Coherent reception, on the other hand, tracks the frequency and phase attributes of the received signal, thus improving receiver sensitivity and selectivity, see [5], [16], [30]. It is for the same reasons that globally optical fiber networks now prefer coherent receivers over direct detection, see [38]–[39]. Fig. 3 illustrates the block diagram of the proposed DP-16 QAM (dual-polarized) multi-hop FSO link in which data is optically modulated, followed by amplification and relayed thereafter over the FSO channel. On the receiver side, the degraded signal from the relay node is band filtered and optically amplified to minimize the effect of the background, thermal and ASE noises. Finally, a coherent detector with the help of a digital signal processor (DSP) performs carrier synchronization for enhanced signal detection. In between the transmitter and the receiver, the relay nodes act as A-F units that perform gain optimization to ensure appropriate signal power levels.

The fundamental principle of DP-16 QAM modulation for optical links can be understood from Fig. 4. The information (bits) is first converted into symbols (4 bits/symbol) by QAM sequence generator followed by M-*ary* pulse generator where these symbols produce a time and amplitude varying equivalent electrical signal. A polarized light source and a pair of Mach Zehnder Modulators (MZM) are then used to generate an optically modulated signal, designated as E_x or E_y, where

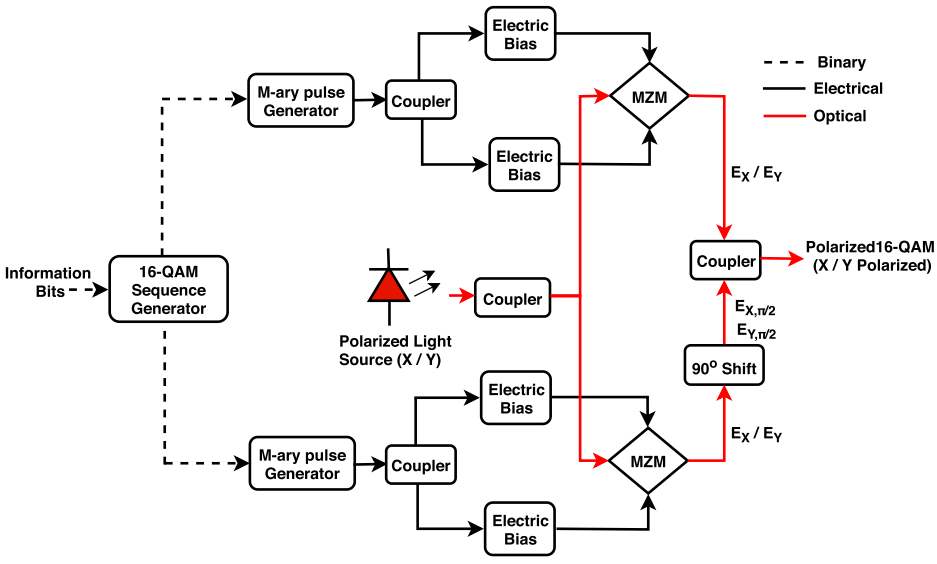

Fig. 4. Simplified illustration of generating optically polarized QAM modulated signal.

subscripts denote the polarization state of the optical source. A phase shift of 90° introduces orthogonality between these two optically modulated versions of the information signal. Polarization combiner later couples these two signals to produce polarized 16-QAM signal and combination of two such polarized 16-QAM signals yields dual-polarized (DP)-16 QAM.

The schematic block diagram of the modulator and demodulator section used in the design of the proposed link are shown in Figs. 5 and 6, respectively. The design elements used in the transmitter of the DP-16 QAM link have been obtained by extrapolating the standard 16-QAM generator shown previously in Fig. 4. Serial to parallel converter divides 120 Gbps information into two bit-streams that are encoded to generate an electrical version of the QAM signal. Later, using an orthogonally polarized light source operating at 193.1 THz (1552.52 nm), Li-Nb Mach Zehnder Modulator (MZM) converts the electrical QAM signal into its optical equivalent. As seen in Fig. 5, the optically modulated signals from MZMs are integrated using 2×1 coupler to yield polarized QAM signal. Polarization combiner later combines the two differently polarized 16-QAM signals, and hence the final output is appropriately known as dual-polarized 16-QAM signal. The reception and decoding process in the QAM receiver follows a very similar reverse pattern. The schematic shown in Fig. 6 is a coherent (homodyne) 16-QAM receiver, which couples a polarized local light source with the incoming optical signal received through the turbulent channel. Four simultaneous optical to electrical conversions are used here to recover the modulated information. Each of these conversion stages is known as balanced detection (B.D). Balanced detectors are known to enhance receiver sensitivity and selectivity by minimising common mode noises, see [38]. The receiver, therefore, witnesses improved signal-to-noise ratio even in the presence of strong fading environments. It is due to these inherent characteristics that coherent detection is anticipated to be highly suited for FSO links operating under adverse atmospheric conditions, see [38], [40]–[42].

Signal detection in the proposed link can be further consolidated by complimenting coherent receivers with digital signal processing (DSP). DSP unit uses a pre-defined algorithm to minimize channel induced impairment factors like distortions in phase, frequency, timing, and polarization. This assertion is based on motivating results reported in, see [30]–[31] about the success of DSP units in mitigating signal information errors and losses in long haul optical fiber links. The signal processing unit used in the proposed link has been designed to ensure: *(i)* timing recovery and blocking D.C noise components *(ii)* adaptive equalization and *(iii)* carrier frequency and phase

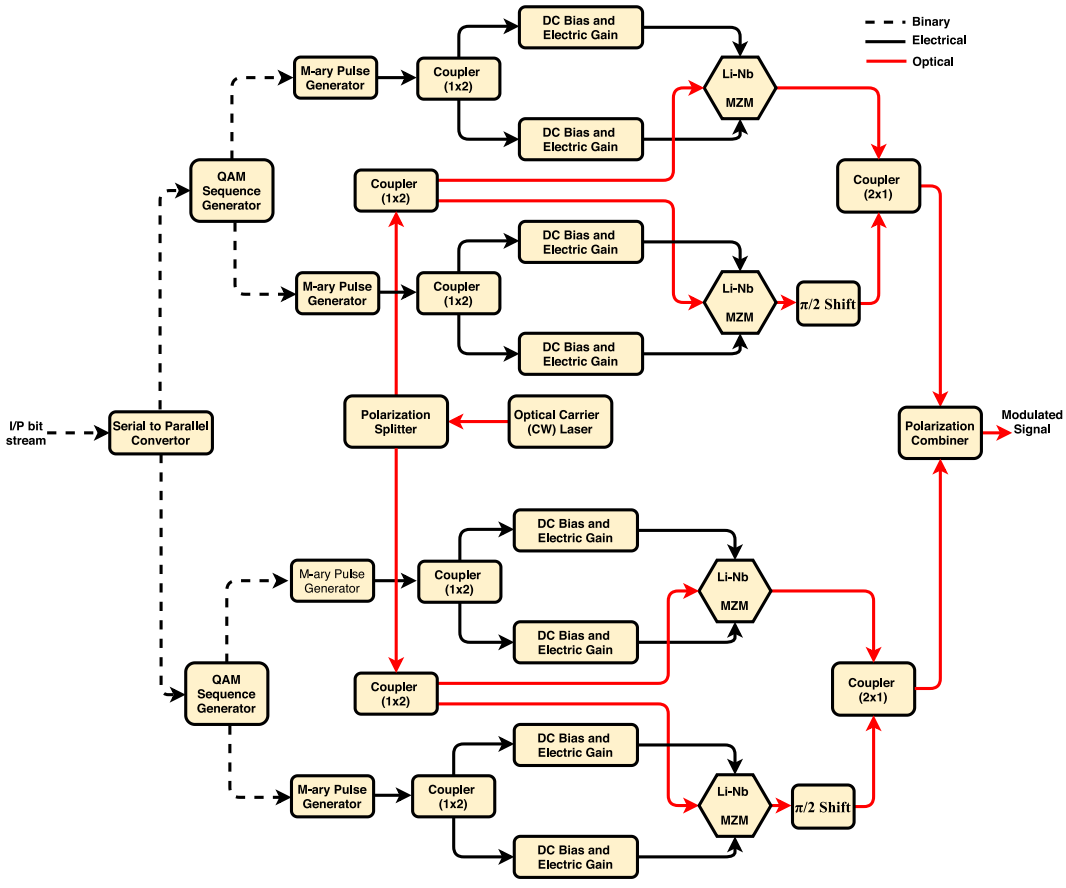

Fig. 5. Block diagram schematic representing modulator section of the proposed link.

estimation for enhanced sensitivity. In the receiver design, the DSP unit is followed by the decision making circuit, which helps in the recovery of in-phase *(I)* and quadrature *(Q)* modulated information bits. The information bits are then re-ordered using parallel to serial *(P/S)* converter to recover modulated information. Since DSP for optical links is already a well-investigated feature, hence interested readers may refer, see [42]–[43] for further elaborations, while detailed information on DSP units used in the proposed link can be found in later sections of this paper.

2.2 Turbulence Theory

On a clear sunny day, when atmospheric visibility is excellent, variation in temperature and pressure along the propagation medium induces beam wandering, beam spreading, and intensity fluctuations, see [3], [5], [7]. Several statistical models like lognormal distribution, K-distribution, and Gamma-Gamma distribution model have been popularly used to quantify the effect of atmospheric turbulence on FSO link performance. However, it is imperative to understand here that while the accuracy of the lognormal distribution is limited to weak turbulence regimes, K-distribution can characterize severe turbulence conditions only, see [1], [5]. As per experimental and analytical literature, see [23]–[25], Gamma-Gamma distribution can model weak to strong turbulence conditions with significant accuracy. For channels characterized using Gamma-Gamma channel distribution, the probability density function (PDF) of received irradiance I is a function of two independent Gamma distributions $f_{(x)}$ and $f_{(y)}$ which are in turn related to the presence of small and large turbulence

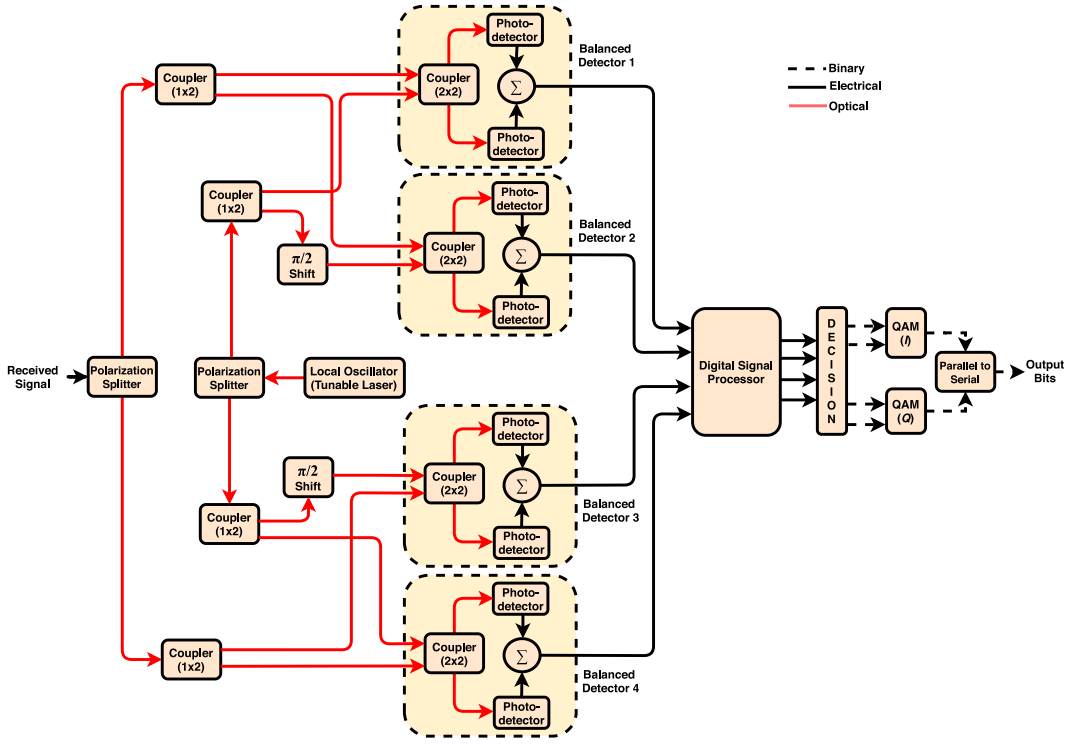

Fig. 6. Block diagram schematic representing receiver section of the proposed link.

eddies, respectively. PDF of received irradiance I, for an otherwise direct FSO link can be expressed as see [3], [6]:

$$f(I) = \frac{2(\alpha\beta)^{(\alpha+\beta)/2}}{\Gamma\alpha\Gamma\beta} I^{\left(\frac{\alpha+\beta}{2}\right)-1} K_{\alpha-\beta}\sqrt{(2\alpha\beta I)} \tag{1}$$

where, $K(.)$ is Bessel function of second order, $\Gamma(.)$ denotes Gamma function while the parameters α and β, signify effects of small and large scale turbulent eddies, respectively. Mathematically, the turbulent eddies α and β are related to intensity fluctuations determined in "(1)" as, see [3], [5], [6]:

$$\alpha = \frac{1}{exp\left[\frac{0.49\sigma^2}{(1+1.11\sigma^{12/5})^{7/6}}\right] - 1} \tag{2}$$

$$\beta = \frac{1}{exp\left[\frac{0.51\sigma^2}{(1+0.69\sigma^{12/5})^{5/6}}\right] - 1} \tag{3}$$

"Equation (1), (2) and (3)," exhibit relation between turbulent eddies and received signal variations. Here $\sigma^2 = 1.23C_n^2 K^{7/6} L^{11/6}$ is the Rytov variance, where $K = 2\pi/\lambda$ represents wave number, L is link distance and λ is operational wavelength. The resulting variance σ^2, represents extent of intensity fluctuations in the received signal. C_n^2 is refractive index structure parameter and symbolically denotes turbulence severity of the propagating medium. More commonly, the numerical values of C_n^2 as 10^{-13} $m^{-2/3}$, 10^{-15} $m^{-2/3}$, 10^{-17} $m^{-2/3}$ are associated with strong, moderate and weak channel turbulent conditions, respectively, see [14], [24]–[25]. For a multi-hop FSO link operating under adverse atmospheric conditions, the probability density functions for

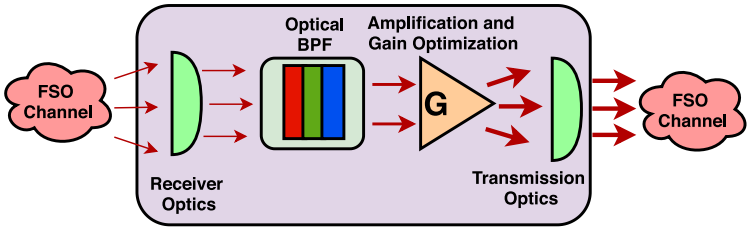

Fig. 7. Internal view of all-optical relay terminal used in proposed link.

Gamma-Gamma modeled link can written by generalizing "(1)" as, see [7], [19]–[20], [25]:

$$f_m(I_{m-1,m}) = \frac{2(\alpha\beta)^{(\alpha+\beta)/2}}{\Gamma\alpha\Gamma\beta} I_{m-1,m}^{(\frac{\alpha+\beta}{2})-1} K_{\alpha-\beta}\sqrt{(2\alpha\beta I_{m-1,m})} \tag{4}$$

"Equation (4)," models probability density function of a multi-hop FSO link between two consecutive serial nodes designated as $(m-1)$ and (m). In triple hop FSO system, refer Fig. 1 for example, the nodes will be designated 0, 1, 2 and 3 wherein the source is treated as node 0 while the destination is indexed as 3. The intermediate serial nodes will be meanwhile designated as node 1 and 2 respectively. Accordingly, variance in case of for multi-hop FSO link can be expressed as, see [25]:

$$\sigma^2 = 1.23 C_n^2 K^{7/6} L_{m-1,m}^{11/6} \tag{5}$$

here, $L_{m-1,m}$ is the link distance between $(m-1)$ and $(m)^{th}$ relay, while rest all the symbols in "(5)" have their usual meaning as explained previously. The expressions in "(4)" and "(5)" can be used to evaluate any n node serial relay FSO link. For the purpose of simplicity, the medium has been considered to be isotropic and turbulence conditions remain static all along the propagation path. The proposed multi-hop link has been evaluated in this paper by contrasting the performance of an otherwise direct link (single hop) with a double and triple hop FSO link. It may be noted that the terminology single relay or double-hop and double relay or triple hop have the same meaning and have been used interchangeably in the subsequent sections of the paper.

2.3 Multi-Hop Serial Transmission

EDFA based amplification for optical fiber links is as of now a very refined technology with extensive research carried out for signal transmission in 1550 nm range, see [44]–[45]. Anticipating similar success, EDFA based amplification has been advocated for optical wireless links as well, see [22], [25], [29], [46]–[47]. Keeping the aforementioned assertions as a basis, we have proposed a multi-hop link with EDFA based amplify-and-forward (A-F) relay mechanism. The internal structure of the all-optical relay nodes used in the proposed link has been highlighted in Fig. 7. Each relay node consists of specialized focusing lenses that are responsible for collecting the optical signal from channel, a band-pass filter (BPF) to remove the effect of background noise and a gain optimized optical amplifier (EDFA). Since each node acts as a amplify-and-forward terminal, hence filtering inside each node ensures minimum noise accumulation even though the signal repeatedly passes through a series of relay terminals. Gain optimization inside relay terminals is essentially a cumulative action of the optical amplifier (EDFA) and gain flattening filter (GFF) optimization. By-product of EDFA action, ASE noise leads to loss of coherence and depleted gain. GFF is a special feature of design tool OptiSystem which is particularly very useful in maximising power transfer with minimum noise amplification while using EDFA for amplification, see [48]. At the other end of relay terminal, transmission lenses form a coherent optical beam which can propagate over free space channel with minimum beam wander. For a serial relay FSO system shown in Fig. 1, assuming that the nodes **S** and **D** are separated by equidistant relay terminals, **R1** and **R2**, the

signal at input of terminal **R1** is mathematically expressed as, see [7], [19], [25]:

$$Y_{R1}(t) = h_{SR1} S_o(t) + n_1(t) \tag{6}$$

here, h_{SR1} is the channel gain for the link between **S** and **R1**, $S_o(t)$ is the original signal transmitted by source node **S**, while $n_1(t)$ is an AWGN noise component with zero mean and power spectral density N_o at node **R1**, see [2], [21]. The signal $Y_{R1}(t)$ is optically amplified inside node **R1** and later propagated over free space channel towards node **R2**. As in "(6)," signal received at node **R2** can be written as, see [25]:

$$Y_{R2}(t) = h_{R1R2}(g_1 Y_{R1}(t) + a_1(t)) + n_2(t) \tag{7}$$

where, h_{R1R2} is the channel gain of link between nodes **R1** and **R2**, g_1 is the amplifier gain of node **R1**, $a_1(t)$ is the noise due to amplification action of EDFA inside node **R1**, while $n_2(t)$ is AWGN noise at node **R2**. After twin hops, the FSO signal makes the last hop to reach the destination node **D**. The signal at this destination node can be expressed as:

$$Y_D(t) = h_{R2D}(g_2 Y_{R2}(t) + a_2(t)) + n_3(t) \tag{8}$$

using "(6)" and "(7)," "(8)" can be simplified and re-written as:

$$Y_D(t) = g_1 g_2 h_{R1R2} h_{R2D}(h_{SR1} S_o(t) + n_1(t)) + g_2 h_{R1R2} h_{R2D}(a_1(t) + n_2(t)) + h_{R2D} a_2(t) + n_3(t) \tag{9}$$

The expression of received signal $Y_D(t)$ deduced in "(9)" can be generalized for any multi-hop FSO link with serial node configuration. It is important to highlight here that as per expression $Y_D(t)$ in "(9)," increasing the number of nodes may not always enhance the link performance to desired levels. This is because amplification inside each node also tends to amplify the channel noise ($n_1(t)$, $n_2(t)$) as well. The noise propagates through the relay nodes towards the destination with further amplification at each stage thus leading to noise accumulation. As highlighted in Fig. 7, a combination of BPF and GFF inside relay ensures that the amplifier gain is optimized to generate sufficient amplification action while minimizing noise accumulation that may occur due to presence of background, thermal and amplifier noise(s). It must be noted here that previous works reported on all-optical A-F relay FSO systems are based on the assumption that the amplifier gain remains fixed throughout all the relay stages. Although convenient in terms of design and analysis but fixed gain stages tend to limit the benefit of multi-hop transmission in FSO links, see [1], [7], [13]–[15], [22]. A practical multi-hop link will require dynamic amplification at each relay terminal which varies as per the link hostilities. The proposed model, therefore, employs EDFA followed by gain optimization to ensure maximum power transfer to the next node. The optimization allows controlling the gain and the output power of the amplifier at each relay terminal individually rather than using predefined and fixed gain across all relays.

2.4 Digital Signal Processing

It is well known fact that direct detection techniques fail miserably to counter turbulence-induced signal fading which in turn leads to erroneous detection, see [1]–[3]. Taking a cue from the success of coherent designs in electronic and RF communication receivers, fiber optical links have also made major headway in reaping benefits from this detection scheme, see [16], [30], [39]–[41]. Moreover recent advances in the field of photonic device design have simplified the inclusion of otherwise complex coherent reception into optical link designs. Coherent detection techniques employ a standard signal source *(local oscillator)* which homodynes with the received signal to recover frequency/phase modulated information. Therefore, such a reception when used in optical wireless links can minimize or even nullify turbulence induced fluctuations of frequency and phase in the received signal, see [5], [30], [49]. In the proposed FSO design the coherent detection is followed by cascading stages of digital signal processing (DSP) units which are collectively responsible for maximizing signal detection even when the channel conditions are extremely disruptive. Positioned between detection and decision making stages as shown in Figs. 6 and 8, the layers of the proposed DSP unit performs filtration, compensation and equalization action

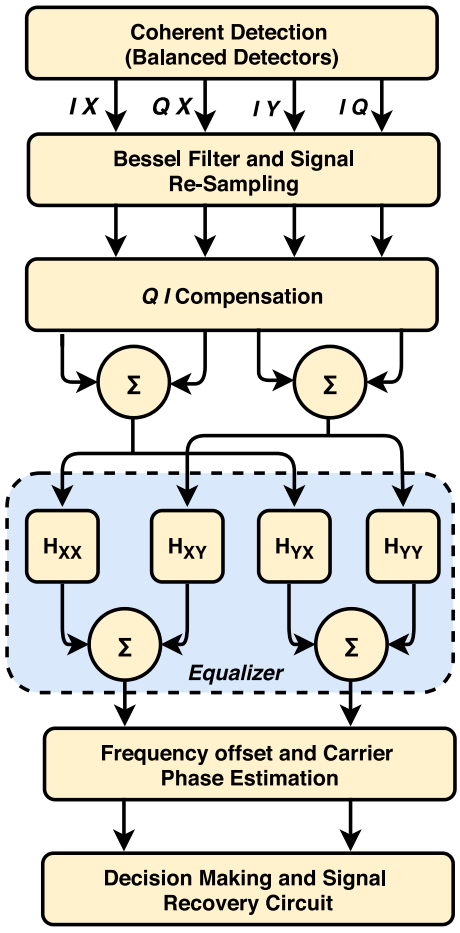

Fig. 8. Block diagram of different modules inside digital signal processing unit.

on the received signal. While coherent detection should help improve receiver sensitivity, the DSP stages will allow compensating waveform distortions thus delivering a cost-effective methodology to enhance link range and capacity in optical wireless links.

The proposed digital signal processing unit houses a fourth-order Bessel filter designed to preserve wave shape of filtered signal especially, when higher-order modulation schemes are used. To enhance the signal resolution, the filtered signal is later re-sampled at the rate of 2 samples per symbol. As explained in previous sections of this paper, since DP- 16 QAM modulated signal is composed of *I* (in-phase) and *Q* (quadrature phase) components of the carrier hence on receiver side it is essential to identify and correct phase imbalances if any, between the two. The imbalances can be attributed to channel adversities and/or faulty receiver characteristics as well. The DSP unit here uses the Gram-Schmidt orthogonalization procedure (GSOP) to compensate for orthogonality errors between *I* and *Q* components of the received signal. The *QI* compensation is followed by constant modulus algorithm-radius based adaptive equalization which uses Butterfly structures to rectify residual noise effects like polarization distortions or phase imbalances in the received signal, see [43], [50]. Any loss of frequency or phase synchronization between local oscillators and the transmitted signal results in frequency shifts in the received signal. This situation leads to inter-carrier interference (ICI) which will be significantly devastating especially in case of high capacity optical wireless links. Based on the principle of estimating signal spectral density, also referred to as maximization of periodogram, frequency offset estimation (FOE) produces requite frequency offsets to synchronize the local and received signal, see [51]. Similarly, phase noise in

TABLE 1
Relation Between Atmospheric Visibility and Link Attenuation

Meteorological Condition	Visibility (km)	Link Attenuation (dB/km)
Clear Weather	> 50	< 1
Haze, Drizzle, Smog	$2 - 20$	$4 - 25$
Severe dust storms	$0 - 0.6$	$40 - 300$

TABLE 2
Different Cases of Link Adversities Considered During the Analysis

Cases	Refractive Index Structure ($m^{-2/3}$)	Link Attenuation (dB/km)
i	$C_n^2 = 10^{-17}$	0.0623
ii		10
iii		25
iv	$C_n^2 = 10^{-13}$	0.0623
v		10
vi		25

the received signal which may be either due to local oscillator, background noise or due to channel adversities, has also been contained in the proposed link by incorporating carrier phase estimation (CPE) into the DSP unit. CPE essentially compensates phase imperfections and is based on low complexity blind phase algorithm, see [50]–[52].

3. Results and Discussions

In this section results obtained from the analysis of the proposed link, illustrated through simulation setups shown in Figs. 3–6, have been presented. Table 1 highlights the relationship between link attenuation (α dB/km) and the impact of meteorological conditions on FSO links operating in 1550 nm window, see [23], [46]. Three different levels of link attenuation (dB/km), 0.063, 10 and 25 have been used to replicate different atmospheric phenomena that may affect the link. In addition to link attenuation, we have also considered an additional loss factor of 5 dB in the overall link budget. This additional loss factor cumulatively accounts for miscellaneous loss factors such as background noise, geometric losses, receiver loss, etc.

Since link attenuation and turbulence-induced fading are individually capable of limiting performance, see [1]–[5], hence it is important that the performance of the proposed link is assessed considering both of the adversaries. Using refractive index structure C_n^2 as metric of turbulence severity, see [7], [30], [53], Table 2 highlights six different channel conditions. *Case (i–vi)* indicate a diverse set of atmospheric conditions for which the performance of the proposed link has been investigated and reported. It must be noted here that during the analysis the relay terminals were placed symmetrically between the source and destination. For example, assuming link length of 1800 meters, triple-hop (double relay) link with equidistant nodes would mean that first relay terminal is placed 600 meters from the source while second relay terminal is placed 1200 meters from the source.

Tables 3 and 4 detail various transmitter and receiver design parameters and their values that have been used to configure the proposed link for multi-hop operation. For link length of 1.8 kms and link parameters tabulated in Tables 3 and 4, Fig. 9 illustrates bit error rate (BER) performance of direct FSO link for all of the six channel conditions *(cases i-vi)* highlighted previously, in Table 2. Evaluated against signal-to-noise ratio, it can be observed from Fig. 9 that severity of turbulence and link attenuation play key role in determining the error performance of the link. In fact, extremely adverse conditions i.e., *case iv-vi*, render direct FSO link completely unsuitable for communication applications due its high BER. However, irrespective of turbulence regime, the error performance of direct link improves as link attenuation eases from 25 dB/km to 0.063 dB/km. Similar investigation

TABLE 3
Proposed Link Transmitter Parameters

Parameter	Value
Modulation Scheme	DP-16 QAM [30],[31]
Data Transmission	$120\ Gbps$ [30],[31]
Length of Sequence	1024 bits [19]
Samples Considered	65536
Laser Type	Continuous Wave (CW)
Optical Transmission Power (P_T)	$-5\ dBm$ to $10\ dBm$ [7],[24],[30]
Modulator	LiNb-MZM
Amplifier Gain (EDFA)	$15\ dB$ [30]
Amplifier Length (EDFA)	$0.5\ meters$ [7]
Pump Characteristics (EDFA)	$980\ nm/100\ mW$/forward
Noise Figure (EDFA)	$6\ dB$ [24]
Transmitter Diameter	$5\ cm$ [7],[9],[14],[30]
Beam Divergence	$2\ mrad$[7],[9],[24],[30]
SMF attenuation @ $1550\ nm$	$0.2\ dB/km$[24]
Wavelength	$193.1\ THz/\ 1552.52\ nm$ [24],[30]

TABLE 4
Proposed Link Channel and Receiver Parameters

Parameter	Value
Link range (L)	Upto $3\ km$ [14],[22]
Additional Link Losses	$5\ dB$ [5]
Channel Fading Model	Gamma-Gamma [7],[14]
Refractive Index Structure (C_n^2)*	10^{-17} and $10^{-13}\ m^{-2/3}$ [5],[14],[22],[24],[30]
Receiver Aperture	$20\ cm$ [7],[14]
Photo detector (PD)	PIN [24]
Receiver Responsivity	$0.9\ A/W$ [19]
Receiver Sensitivity	$-16\ dBm$ [24]
Dark Current	$10\ nA$ [30]
Shot Noise	$5\ nA$
Thermal Power Density	$100^{-24}\ W/Hz$
Absolute Temperature at Receiver	$298\ Kelvin$[22]
Load Resistance	$50\ ohm$ [22]
Junction Capacitance	$3\ pF$
Local Oscillator Pump power	$10\ dBm$ [30]

* 10^{-17} and 10^{-13} denote refractive index structure for weak and strong turbulence conditions respectively.

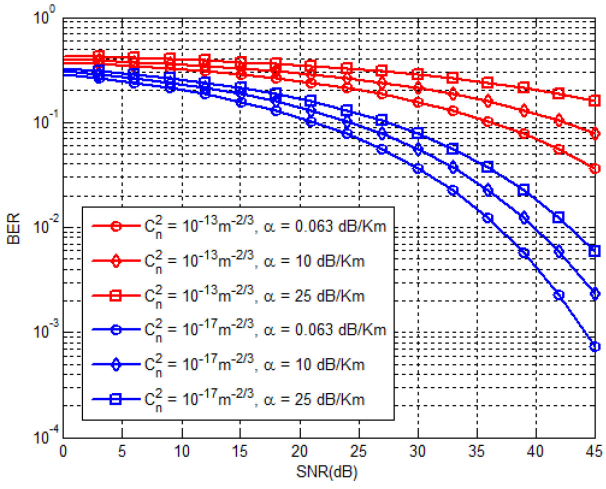

Fig. 9. BER versus SNR pattern of direct FSO link for different link conditions.

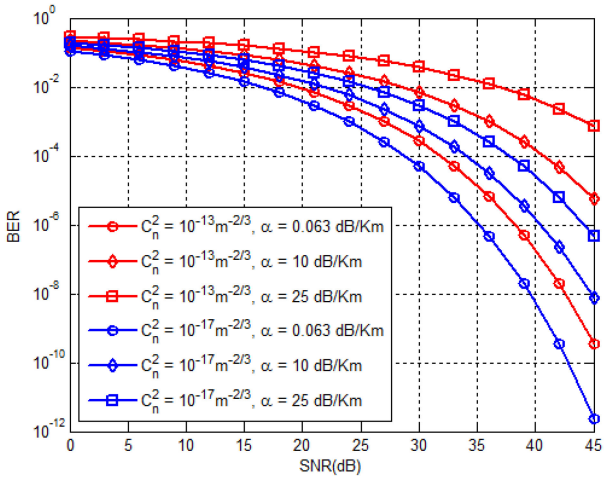

Fig. 10. BER versus SNR pattern of double-hop FSO link for different link conditions.

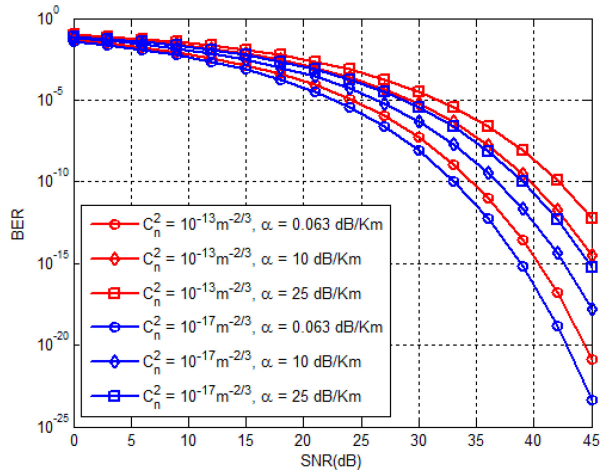

Fig. 11. BER versus SNR pattern of triple-hop FSO link for different link conditions.

on error performance of double-hop link has been highlighted in Fig. 10. Considering the *case iv*, i.e., when $C_n^2 = 10^{-13}\ m^{-2/3}$ and $\alpha = 0.063$ dB/km, it can be observed from Figs. 9 and 10 that at reference SNR of 35 dB, BER improves from 10^{-1} (approx.) in direct link to 10^{-5} (approx.) in double-hop link, thus resulting in BER improvement of four orders. Likewise, for *case i*, i.e., when $C_n^2 = 10^{-17}\ m^{-2/3}$ and $\alpha = 0.063$ dB/km, BER again improves by approximately four orders of magnitude in double-hop links when compared with the direct link. Comparison of BER as observed from Figs. 9 and 10 present a notion that dividing the link into smaller segments aids in limiting channel losses thus reducing the overall BER.

Extending the investigation, Fig. 11 reveals error performance of triple-hop FSO link. For strong turbulence conditions i.e., *case vi*, at receiver SNR of 35 dB the observed BER patterns are: while direct FSO experiences almost complete link impairment with BER of 10^{-1}, which reduces to 10^{-2} for double-hop and finally 10^{-6} for triple-hop configuration. For *case iii*, wherein weak turbulence ($C_n^2 = 10^{-17}$) is accompanied with link attenuation of 25 dB/km, BER improves from 10^{-2} to 10^{-4} and then to 10^{-7} for direct, double-hop and triple-hop FSO link respectively. Table 5 shows vis-a-vis BER comparison of different link configurations as observed from Figs. 9 – 11.

TABLE 5
BER (Approx.) Comparison of Multi-Hop FSO Links With Direct Link for Different Channel Conditions (Reference SNR 35 dB)

Link Type	$C_n^2 = 10^{-17}\, m^{-2/3}$			$C_n^2 = 10^{-13}\, m^{-2/3}$		
	α= 0.063dB/km	α= 10 dB/km	α= 25 dB/km	α=0.063dB/km	α = 10 dB/km	α= 25 dB/km
Direct Link	10^{-2}	10^{-2}	10^{-2}	10^{-1}	10^{-1}	10^{-1}
Double-Hop	10^{-6}	10^{-4}	10^{-3}	10^{-5}	10^{-3}	10^{-1}
Triple-Hop	10^{-12}	10^{-9}	10^{-7}	10^{-10}	10^{-7}	10^{-6}

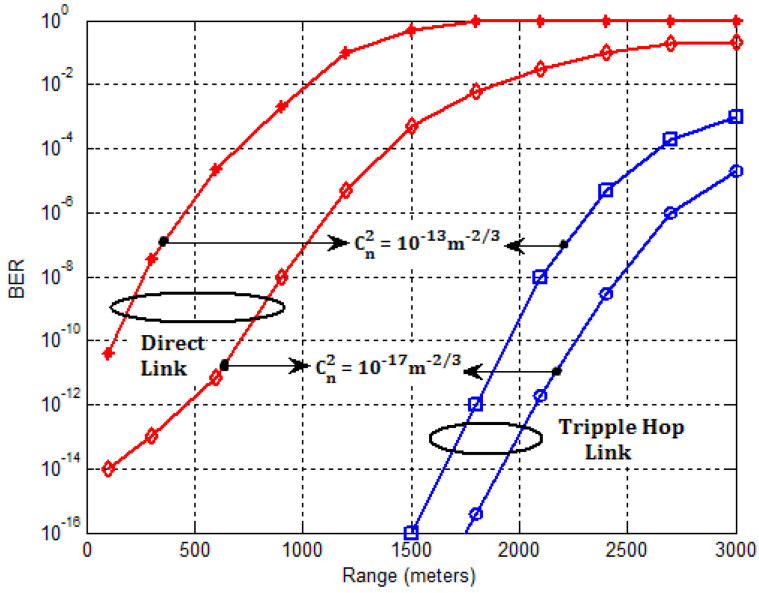

Fig. 12. BER comparisons of direct and triple-hop FSO link for varying link range.

Another important observation from Figs. 9–11 and subsequently Table 5 is about the convergence of BER performances of multi-hop FSO links over different channel conditions. While the BER curve patterns in case of direct link for different link conditions stay distinctly separated as seen in Fig. 9, significant overlapping of curves can be seen for multi-hop transmission in Figs. 10 and 11. As the numbers of hops are increased from 0 to 3, BER performance under different channel conditions shows a greater degree of similarity and it appears that as if the impact of channel conditions on link performance has normalized. The reason for the convergence of BER can be attributed to the fact that as the number of relay terminals are increased, the percentage decrease of distance between two adjacent nodes begins to decrease. For example, consider a link where the source and the destination are 1500 meters apart. The introduction of symmetric relay node will now reduce between any two consecutive nodes to 750 meters, i.e., 50% decrease in distance. However, if the same link is now replaced with symmetrically placed twin relays (triple-hop), then the distance between any two consecutive nodes will now reduce from 750 meters previously to 500 meters. Therefore, the introduction of the additional node means that the inter-node distance in triple-hop link reduces by 33.3% compared to 50% reduction witnessed by double-hop link. Thus by extending this analogy it can be concluded that as the numbers of nodes increase the link BER performance will witness saturation as the percentage decrease of distance between two consecutive nodes becomes more and more nominal.

Apart from the analysis of link performance in terms of BER, the proposed link has also been investigated for possible link range increment that can be achieved with multi-hop arrangement. Fig. 12 evaluates the BER performance of the proposed multi-hop FSO link for different link

TABLE 6
Approximate Link Range in Meters of the Proposed Link for Different Reference Values of BER

Link Type	C_n^2 $(m^{-2/3})$	**Link Range (met.) (BER**$= 10^{-5}$**)**	**Link Range (met.) (BER**$= 10^{-12}$**)**
Direct Link	10^{-17}	1160	< 500
	10^{-13}	570	< 500
Triple Hop	10^{-17}	2690	1800
	10^{-13}	2240	2040

range. Since it has now been emphatically established from Figs. 9–11 and Table 5 that triple-hop FSO link results in superior error performance over double-hop and direct FSO links. Hence, our investigation on BER performance for varying link shown in Fig. 12 is confined to the triple-hop link and its comparison with standard direct links.

The aforementioned analysis has been carried out at reference receiver SNR of 45 dB while the link conditions correspond to *case iii* and *case vi* of Table 2. Analysis of Fig. 12 reveals that at target BER of 10^{-5}, the communication link range of 2440 meters and 570 meters can be achieved for triple-hop and direct link respectively. Multi-hop arrangement therefore results in an excellent range increment of 1870 meters (1.870 km) over direct FSO link. The detailed comparison of approximate link ranges for different reference BER's over varied turbulence regimes can be seen in Table 6. Apart from proposing the futuristic applications of multi-hop link that can support societal needs, the demonstrated link has also been designed and investigated to achieve performance enhancement over previously reported literature on high-speed FSO connectivity, see [30]. At BER of 10^{-12}, see [30] reported an achievable link range of 1.1 km over moderate turbulence regime $C_n^2 = 10^{-15}$ $m^{-2/3}$. However, it can be observed in Fig. 12 and Table 6 that our proposed link efficiently enhances the link range to 1.80 km and 2.04 km respectively over strong (10^{-13} $m^{-2/3}$) and weak turbulence (10^{-17} $m^{-2/3}$) regimes respectively. Thus, despite the turbulence considered in the proposed link being severe than the one reported in, see [30], the proposed triple-hop link enhances the useful link range by approximately 700 meters when compared to, see [30]. Miscellaneous observed advantages of the proposed link include a major reduction in optical transmission power levels. Against 20 dBm of transmission power reported in, see [30], the proposed link could operate efficiently with optical power ranging from -5 dBm to 10 dBm. Considering design costs and complexities, such a magnitude of reduction in transmission power will be critical in expediting convergence between backbone optical networks and FSO links.

Additionally, the use of hybrid RF/FSO links for smart city applications has been detailed in, see [54]. However, under strong turbulence conditions the reported link [54] fails to deliver, prompting the use of low capacity RF link as backup. Depending upon the link conditions, the transmitter will switch between optical and low capacity RF carrier. Not only does this arrangement bring in design complexities but it may also leave end-users dissatisfied due to abrupt data speeds and frequent loss connectivity during switching transitions. The proposed link is however observed to do exceedingly well in delivering optical bandwidth to end users even under extremely adverse conditions and that too without any additional requirement of cost-intensive optoelectronic amalgamation. Authors strongly believe that being an all-optical configuration the proposed multi-hop FSO link will suit cost-effective and hassle-free integration with existing optical access networks.

Digital signal processing facilitates timing recovery, equalization and carrier frequency estimation (CPE) followed by frequency offset estimation (FOE), thus playing a significant role in improving error performance of the link. Figs. 13 and 14 illustrates constellation diagrams of the proposed link recorded at different stages of the digital signal processing (DSP) unit. As seen in Figs. 13(a) and 14(a), the constellation points are overwhelmingly overlapping and congested while the condition is far worse in the latter's case (10^{-13} $m^{-2/3}$). As the received signal passes through different stages of the DSP module which includes equalization, CPE and FOE, remarkable improvement can be seen. In Figs. 13(c) and 14(c), the constellation points are discreetly visible which vindicates our

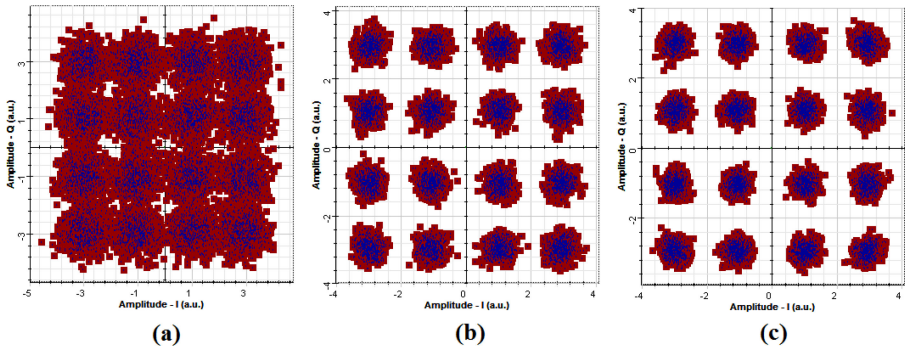

Fig. 13. Constellation diagrams of proposed link recorded after (a) equalization (b) FOE and (c) CPE, when $C_n^2 = 10^{-17} m^{-2/3}$, $\alpha = 25$ dB/Km, $P_T = 5dBm$ and $L_T = 1.5$ km.

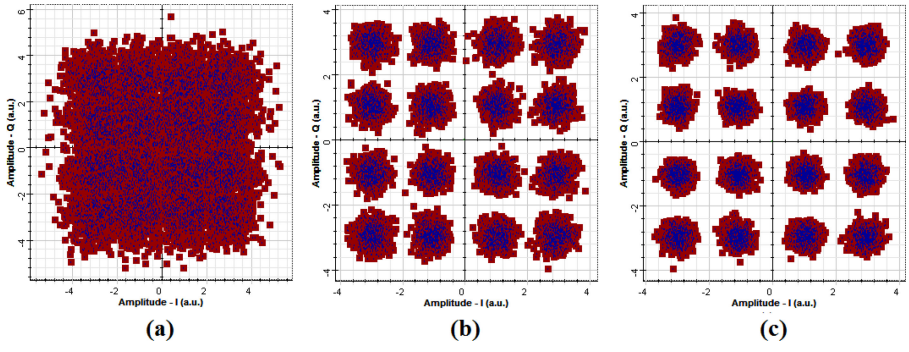

Fig. 14. Constellation diagrams of proposed link recorded after (a) equalization (b) FOE and (c) CPE, when $C_n^2 = 10^{-13} m^{-2/3}$, $\alpha = 25$ dB/Km, $P_T = 5dBm$ and $L_T = 1.5$ km.

assertion that DSP can assist in overcoming channel induced losses. While overlapping constellation points result in erroneous symbol detection, separated points on the other hand yield reliable information detection. Therefore, it can be conclusively said that the DSP unit can successfully mitigate the effect of turbulence-induced signal fading which in turn improves BER of the link. To further strengthen the conviction on novelty, Table 7 holistically compares the performance of the proposed link with six contemporary works on 8 different parameters. Some notable outcomes of this comparison are: *(i)* the proposed link has been investigated for array adverse channel conditions while the same is either missing or too nominal in reported literature, *(ii)* the proposed link is found to deliver decent link range which provisions cost-effective last-mile connectivity, *(iii)* with its novel features like coherent detection, DSP and multi-hop relay, the proposed link achieves link range and data capacity which is practically the best amongst compared literature and *(iv)* being an all-optical configuration, the proposed high capacity link can easily integrate with existing backbone networks to deliver data services to remote and inaccessible areas.

Interestingly, as per various available statistics, despite being within 1-mile distance from fiber backbone networks, 75 percent businesses in even developed countries like the USA do not have access to optical bandwidth. High costs, lengthy setup and installation time are the key reason for such low penetration of optical fiber. FSO links on the other hand can be set up on $1/10^{th}$ of cost it takes to install fiber connectivity while the time span is merely $1-7$ days, see [1]–[2], [6], [55], [56]. In such a scenario, the proposed link with a serviceable range of up to 2.2 kms can potentially serve as cost-effective and high-speed access for solving last-mile issues in delivering optical bandwidth to end-users.

TABLE 7
Comparison of Proposed Link Performance With Recent Research Work

Comparison Parameter	[30]	[33]	[34]	[36]	[57]	[58]	Proposed Design	Remarks
Link Attenuation	25 dB/km	0.064-85.5 dB/km	0.065-2.37 dB/km	6.2-96.8 dB/km	0.22 dB/km	0.43-4.8 dB/km	0.063-25 dB/km + 5 dB	Link investigated for various practical atmospheric conditions.
Turbulence Modelling	Yes	Yes	No	No	Yes	No	Yes	Fading effect of channel has also been considered.
Turbulence Severity	Moderate	Weak to Strong	N.A	N.A	Weak to Strong	N.A	Weak to Strong	Link tested for extreme channel conditions.
Optical Transmission Power	20 dBm	10 dBm	10-40 dBm	10 dBm	5 dBm	10 dBm	-5-10 dBm	Human safety and practically realizable transmission power level considered.
Date Rate	120 $Gbps$	80 $Gbps$	2.5 $Gbps$	10 $Gbps$	10 $Gbps$	1.25 $Gbps$	120 $Gbps$	High-speed connectivity for last-mile applications.
DSP Unit	Yes	No	No	No	No	No	Yes	Enhanced signal recovery through coherent detection and carrier synchronization.
Link Range	1.1 km	0.5-35 km	47-950 km	1.7-16.5 km	150 km	1 km	1.80-2.04 km	Reasonable and realistic range for last-mile solutions.
Gain Optimization	No	Yes	No	No	No	No	Yes	Descent optical power at each node while assuring lower noise accumulation due to EDFA's.

4. Limitations and Constraints

The novelty of the proposed multi-hop transmission lies with the introduction of an optical relay mechanism which can by virtue of its design support high speed signal processing. Contrary to the conventional hardware equipment which convert optical signal to equivalent photocurrent to decode and regenerate the signal, the proposed architecture will have higher setup cost factor. However, considering the dynamic adaptability of system to integrate with high speed backbone networks, the cost factor should average out in long run i.e., cost/Mbps/month. Additionally, relays use EDFA for all optical amplification, hence optical wireless links operating in visible band, which have also gained significant popularity, will be incompatible with the proposed architecture. Lastly, as observed from the results, increase in number of relays causes power gain saturation which in turn causes the BER performance of different relay configurations to converge. Therefore, a thoughtful trade-off between number of relays and expected performance must be drawn as each extra relay will not only significantly add to link cost and but also lead to design complexities.

5. Conclusion

In this paper all-optical amplify-and-forward multi-hop transmission has been considered as a promising solution for enhancing the performance of 120 Gbps DP-16 QAM FSO link. The investigations have been carried for a variety of atmospheric channel conditions ranging from mild to severe. BER analysis of the proposed multi-hop relay assisted FSO link has been accomplished

over the fading channel and the results have then been compared with direct link. Our investigations reveal that multi-hop transmission with relays placed symmetrically between source and receiver, experience phenomenal improvement in communication range and BER performance. For double-hop link and at reference SNR of 35 dB, the BER improved by four orders of magnitude over direct FSO link. Similarly, at target BER of 10^{-5} the communication link range witnessed increment of 1.87 km over direct FSO link. Further, at target BER of 10^{-12}, the proposed relay assisted FSO link significantly improved the link range to approximately 1.8 km as compared to 1.1 km reported in the recent literature. Additionally, use of multi-hop relay allowed reduction of transmission power levels to 10 dBm in comparison to 20 dBm reported in the literature. The proposed triple-hop link delivers appreciable link range in excess of 1.5 km over different turbulence regimes with very nominal transmission power. It is thus concluded that link range of such magnitude is suitable enough to cater to needs to last-mile connectivity as well as remote delivery of medical consultation and tele-medicine applications.

The reported research can be further extended to designing an mesh link network where the nodes can intelligently choose the optimum propagation path. Aided with artificial intelligence these nodes should anticipate channel conditions over given link and set its priorities accordingly.

Acknowledgment

We would like to thank chief editor, editor, and anonymous reviewers for their valuable reviews.

References

[1] A. K. Majumdar, Z. Ghassemlooy, and A. A. B. Raj, *Principles and Applications of Free Space Optical Communications*. London, United Kingdom: Institution of Engineering and Technology, 2019, pp. 1–330.
[2] A. K. Majumdar, *Advanced Free Space Optics (FSO): A System Approach*. Ridgecrest, CA, USA: Springer, 2015, pp. 21–173.
[3] Z. Ghassemlooy, W. Popoola, and S. Rajbhandari, *Opt. wireless communications: System and channel modelling with MATLAB*. Boca Raton, FL, USA: CRC Press Taylor and Francis Group, 2013, pp. 1–30.
[4] A. K. Majumdar, *Optical Wireless Communications for Broadband Global Internet Connectivity: Fundamentals and Potential Applications*. Cambridge, MA, USA: Elsevier, 2018, pp. 39–52.
[5] M. A. Khalighi and M. Uysal, "Survey on free space optical communication: A communication theory perspective," *IEEE Commun. Surv. Tut.*, vol. 16, no. 4, pp. 2231–2258, Oct./Dec. 2014.
[6] Q. Liu *et al.*, "Optical wireless communication networks for first-and last-mile broadband access," *J. Opt. Netw.*, vol. 4, no. 12, pp. 807–828, 2005.
[7] N. A. M. Nor, Z. Ghassemlooy, S. Zvanovec, M. Khalighi, and M. R. Bhatnagar, "Comparison of optical and electrical based amplify-and-forward relay-assisted FSO links over gamma-gamma channels," in *Proc. Int. Symp. Commun. Syst., Netw. Digit. Signal Process.*, 2016, pp. 1–5.
[8] K. O. Odeyemi, P. A. Owolawi, and V. M. Srivastava, "Performance analysis of decode-and-forward dual-hop optical spatial modulation with diversity combiner over atmospheric turbulence," *Opt. Commun.*, vol. 402, pp. 242–251, 2017.
[9] P. V. Trinh, N. T. Dang and A. T. Pham, "Optical amplify-and-forward multihop WDM/FSO for all-optical access networks," in *Proc. 9th Int. Symp. Commun. Syst., Netw. Digit. Signal Process.*, 2014, pp. 1106–1111.
[10] Y. Arimoto, "Compact free-space optical terminal for multi-gigabit signal transmission with a single mode fiber," in *Proc. SPIE*, San Jose, CA, USA, 2009, vol. 7199, no. 7, pp. 1–9.
[11] H. Kaushal and G. Kaddoum, "Optical communication in space: Challenges and mitigation techniques," *IEEE Commun. Surv. Tut.*, vol. 19, no. 1, pp. 57–96, Jan.-Mar. 2017.
[12] J. Perez, S. Zvanovec, Z. Ghassemlooy, and W. O. Popoola, "Experimental characterization and mitigation of turbulence induced signal fades within an ad hoc FSO network," *Opt. Express*, vol. 22 no. 3, pp. 3208–3218, 2014.
[13] M. A. Kashani, M. M. Rad, M. Safari and M. Uysal, "All-optical amplify-and-forward relaying system for atmospheric channels," *IEEE Commun. Lett.*, vol. 16, no. 10, pp. 1684–1687, Oct. 2012.
[14] S. Kazemlou, S. Hranilovic, and S. Kumar, "All-optical multihop free-space optical communication systems," *J. Lightw. Technol.*, vol. 29, no. 18, pp. 2663–2669, Sep. 2011.
[15] M. Safari and M. Uysal, "Relay-assisted free-space optical communication," *IEEE Trans. Wireless Commun.*, vol. 7, no. 12, pp. 5441–5449, Dec. 2008.
[16] Y. Wang, D. Wang, and J. Ma, "On the performance of coherent OFDM systems in free-space optical communications," *IEEE Photon. J.*, vol. 7, no. 4, Aug. 2015, Art. no. 7902410.
[17] L. Yang X. Gao, and M. S. Alouini, "Performance analysis of free-space optical communication systems with multiuser diversity over atmospheric turbulence channels," *IEEE Photon. J.*, vol. 6, no. 2, Apr. 2014, Art. no. 7901217.
[18] Z. Wang, W.-D. Zhong, S. Fu, and C. Lin, "Performance comparison of different modulation formats over free-space optical (FSO) turbulence links with space diversity reception technique," *IEEE Photon. J.*, vol. 1, no. 6, pp. 277–285, 2009.

[19] N. A. M. Nor, Z. Ghassemlooy, S. Zvanovec, and M. Khalighi, "Performance analysis of all-optical amplify-and-forward FSO relaying over atmospheric turbulence," in *Proc. IEEE Student Conf. Res. Develop.*, 2015, pp. 289–293.
[20] N. A. M. Nor *et al.,* "10 Gbps all-optical relay-assisted FSO system over a turbulence channel," in *Proc. 4th Int. Workshop Opt. Wireless Commun.*, 2015, pp. 69–72.
[21] T. V. Pham and A. T. Pham, "Performance analysis of amplify–decode-and-forward multihop binary phase-shift keying/free-space optical systems using avalanche photodiode receivers over atmospheric turbulence channels," *IET Commun.*, vol. 8, no. 9, pp. 1518–1526, 2014.
[22] E. Bayaki, D. S. Michalopoulos, and R. Schober, "EDFA-based all optical relaying in free-space optical systems," *IEEE Trans. Commun.*, vol. 60, no. 12, pp. 3797–3807, Dec. 2012.
[23] J. Libich, M. Komanec, S. Zvanovec, P. Pesek, W. O. Popoola, and Z. Ghassemlooy, "Experimental verification of an all-optical dual-hop 10 Gbit/s free-space optics link under turbulence regimes," *Opt. Lett.*, vol. 40, no. 3, pp. 391–394, 2015.
[24] N. A. M. Nor *et al.*, "Experimental investigation of all-optical relay-assisted 10 Gb/s FSO link over the atmospheric turbulence channel," *J. Lightw. Technol.*, vol. 35, no. 1, pp. 45–53, Jan. 2017.
[25] M. Atakora and H. Chenji, "A multicast technique for fixed and mobile optical wireless backhaul in 5G networks," *IEEE Access*, vol. 6, pp. 27491-27506, 2018.
[26] T. S. Rappaport *et al.*, "Wireless communications and applications above 100 GHz: Opportunities and challenges for 6G and beyond," *IEEE Access*, vol. 7, pp. 78729–78757, 2019.
[27] M. Atakora and H. Chenji, "A multicast technique for fixed and mobile optical wireless backhaul in 5G networks," *IEEE Access*, vol. 6, pp. 27491–27506, 2018.
[28] G. Parca, A. Shahpari, V. Carrozzo, G. M. T. Beleffi, and A. L. J. Teixeira, "Optical wireless transmission at 1.6-Tbit/s (16×100 Gbit/s) for next-generation convergent urban infrastructures," *Opt. Eng.*, vol. 52, no. 11, pp. 116102–116105, 2013.
[29] X. Huang *et al.*, "WDM Free-space optical communication system of high-speed hybrid signals," *IEEE Photon. J.*, vol. 10, no. 6, pp. 1–7, Nov. 2018.
[30] D. Kakati and S. C. Arya, "A full-duplex optical fiber/wireless coherent communication system with digital signal processing at the receiver," *Optik*, vol. 171, pp. 190–199, 2018.
[31] D. Kakati and S. C. Arya, "Performance of 120 Gbps Single Channel Coherent DP-16-QAM in Terrestrial FSO Link under Different Weather Conditions," *Optik*, vol. 178, pp. 1230–1239, 2019.
[32] E. Ciaramella *et al.*, "1.28 Terabit/s (32×40 Gbit/s) WDM transmission system for free space optical communications," *IEEE J. Sel. Areas Commun.*, vol. 27, no. 9, pp. 1639–1645, Dec. 2009.
[33] N. Badar, R. K. Jha, and Towfeeq, "Performance analysis of an 80 (8×10) Gbps RZ-DPSK based WDM-FSO system under combined effects of various weather conditions and atmospheric turbulence induced fading employing Gamma–Gamma fading model," *Opt. Quant. Electron.*, vol. 50, no. 44, pp. 1–11, 2018.
[34] A. Malik and P. Singh, "Comparative Analysis of Point to Point FSO System Under Clear and Haze Weather Conditions," *Wireless Pers. Commun.*, vol. 80, no. 2, pp. 483–492, 2015.
[35] M. Grover *et al.*, "Multibeam WDM-FSO System: An Optimum Solution for Clear and Hazy Weather Conditions," *Wireless Pers. Commun.*, vol. 97, no. 4, pp. 5783–5795, 2017.
[36] M. Singh, "Performance analysis of WDM-FSO system under adverse weather conditions," *Photon. Netw. Commun.*, vol. 36, no. 1, pp. 1–10, 2018.
[37] H. Hsu, W. C. Lu, H. L. Minh, Z. Ghassemlooy, Y. Yu, and S. Liaw, "2×80 Gbit/s DWDM bidirectional wavelength reuse optical wireless transmission," *IEEE Photon. J.*, vol. 5, no. 4, pp. 7901708–7901708, 2013.
[38] H. Yao *et al.*, "Performance analysis of MPSK FSO communication based on the balanced detector in a fiber-coupling system," *IEEE Access*, vol. 7, pp. 84197–84208, 2019.
[39] M. Yoshida, H. Goto, K. Kasai, and M. Nakazawa, "64 and 128 coherent QAM optical transmission over 150 km using frequency-stabilized laser and heterodyne PLL detection," *Opt. Exp.*, vol. 16, no. 2, pp. 829–840, 2008.
[40] L. Li *et al.*, "Free-space optical communication using coherent detection and double adaptive detection thresholds," *IEEE Photon. J.*, vol. 11, no. 1, pp. 1–17, Feb. 2019.
[41] R. Zhang *et al.*, "Full-duplex fiber-wireless link with 40 Gbit/s 16-QAM signals for alternative wired and wireless accesses based on homodyne/heterodyne coherent detection," *Opt. Fiber Technol.*, vol. 20, no. 3, pp. 261–267, 2014.
[42] D.-S. Ly-Gagnon, K. Katoh, and K. Kikuchi, "Unrepeated 210-km transmission with coherent detection and digital signal processing of 20-Gb/s QPSK signal," in *Proc. OFC/NFOEC Tech. Digest. Opt. Fiber Commun. Conf.*, 2005, pp. 1–3.
[43] S. J. Savory, "Digital filters for coherent optical receivers," *Opt. Express*, vol. 16, no. 2, pp. 804–817, 2008.
[44] T.-C. Liang, C.-H. Chang, and Y.-K. Chen, "Optimum configuration and characteristic comparisons of multiwavelength erbium-doped fiber amplifier for hybrid digital/analog WDM systems," *Opt. Commun.*, vol. 177, nos. 1-6, pp. 259–269, 2000.
[45] C. R. Giles and E. Desurvire, "Modeling erbium-doped fiber amplifiers," *J. Lightw. Technol.*, vol. 9, no. 2, pp. 271–283, Feb. 1991.
[46] M. A. Esmail, A. M. Ragheb, H. A. Fathallah, M. Altamimi, and S. A. Alshebeili, "5G–28 GHz signal transmission over hybrid all-optical FSO/RF link in dusty weather conditions," *IEEE Access* , vol. 7, pp. 24404–24410, 2019.
[47] L. Li *et al.*, "Free-space optical communication using coherent detection and double adaptive detection thresholds," *IEEE Photon. J.*, vol. 11, no. 1, pp. 1–17, Feb. 2019.
[48] "Gain Flattening Filter Optimization," Optiwave, 2020. [Online]. Available: https://optiwave.com/resources/applications-resources/optical-system-gain-flattening-filter optimization Accessed: 07- Mar.- 2020.
[49] X. Tang, Z. Ghassemlooy, S. Rajbhandari, W. O. Popoola, and C. G. Lee, "Coherent optical binary polarisation shift keying heterodyne system in the free-space optical turbulence channel," *IET Microw., Antennas Propag.*, vol. 5, no. 9, pp. 1031–1038, 2011.
[50] I. Fatadin D. Ives, and S. J. Savory, "Blind equalization and carrier phase recovery in a 16-QAM optical coherent system," *J. Lightw. Technol.*, vol. 27, no. 15, pp. 3042–3049, Aug. 2009.

[51] P. Ciblat and L. Vandendorpe, "Blind carrier frequency offset estimation for non-circular constellation based transmission," *IEEE Trans. Signal Process.*, vol. 51, no. 5, pp. 1378–1389, May 2003.
[52] E. Pincemin, N. Brochier, M. Selmi, O. Z. Chahabi, P. Ciblat, and Y. Jaouën, "Novel blind equalizer for coherent DP-BPSK transmission systems: theory and experiment," *IEEE Photon. Technol. Lett.*, vol. 25, no. 18, pp. 1835–1838, Aug. 2013.
[53] A. K. Majumdar and J. C. Ricklin, *Free-Space Laser Communications: Principles and Advances*. New York, USA: Springer, 2008.
[54] P. Krishnan, "Performance analysis of hybrid RF/FSO system using BPSK-SIM and DPSK-SIM Over gamma-gamma turbulence channel with pointing errors for smart city applications," *IEEE Access*, vol. 6, pp. 75025–75032, 2018.
[55] V. Ramasarma, "Free space optics, a viable last-mile solution," *Bechtel Telecommun. Tech. J.*, vol. 1, pp. 22–30, 2002.
[56] A. K. Majumdar, *Optical Wireless Communications for Broadband Global Internet Connectivity: Fundamentals and Applications*. Amsterdam, Netherlands: Elsevier, 2019, pp. 39–53.
[57] N. Badar and R. Kumar Jha, "Performance comparison of various modulation schemes over free space optical (FSO) link employing Gamma–Gamma fading model," *Opt. Quantum Electron.*, vol. 49, no. 5, pp. 192(1–10), 2017.
[58] G. Immadi *et al.*, "Estimating the performance of free space optical link under adverse weather conditions by using various models," *Wireless Pers. Commun.*, vol. 103, no. 2, pp. 1603–1613, 2018.